Prediction of current and potential distributions on galvanic corrosion by boundary element method

F.E. Varela,[a] Y. Kurata,[b] N. Sanada[b]

[a]*Instituto de Investigaciones Fisicoquimicas Teoricas y Aplicadas (INIFTA), UNLP, Suc. 4 - CC 16, (1900) La Plata, Argentina*

[b]*Tohoku National Industrial Research Institute (TNIRI), AIST, Nigatake 4-2-1, Miyagino-ku, Sendai, 983, Japan*

Abstract

Distributions of current density and potential have been analyzed on a carbon steel (SS400) - stainless steel (SUS304) couple. General and galvanic corrosion results were experimentally obtained in NaCl solution for different temperatures and immersion times. The experimentally determined polarization curves defined the nonlinear boundary conditions of the Laplace's equation and numerical results have been calculated using the boundary element method. The influence of the elementary spacing and thickness as well as the effect of insulating materials in the galvanic model have been analyzed.

1 Introduction

The risk of galvanic corrosion often justifies a warning against combinations of dissimilar metals in corrosive environments. The corrosion is stimulated by the potential difference that exists between the two metals, the more noble acting as a cathode where some oxidizing species is reduced, the more active metal, which corrodes, acting as the anode. The corrosion rates and the potential distribution over a galvanic couple depend upon the electrochemical properties of the metals, on environmental variables such as temperature, salinity, oxygen content, and solution flow, as well as the geometry of the corroding system. However, a galvanic coupling does not always lead to significant attack or to an unacceptable degree of corrosion[1]. The severity of attack depends on the conditions. If dissimilar materials can be coupled without significant damage, a greater flexibility in the material selection may be possible. This can be done only if the galvanic corrosion rates can be predicted by calculation and/or experimental models.

The literature reports several cases in which calculation of current distribution and potential variation using analytical or numerical methods were utilized. Analytical solutions have been described by Waber *et al.*[2,3]. Numerical methods are more flexible for various geometries and polarization behaviours. The finite

difference method has been used for calculation of potential variation and current distribution[4,5]. In addition, the finite element method has also been used[6,7]. A particularly promising method is the boundary element method, which was introduced for cathodic protection systems[8,9] and recently for galvanic current distribution calculations[10,11].

The aims of this work are: (1) to develop and use an experimental model to measure the current distribution over the coupled surfaces; and (2) to predict by numerical calculation the potential and current distributions on a galvanic couple. This mathematical modelling can provide a means of verification and accurate evaluation on galvanic corrosion data from the knowledge of the corrosion behaviour of the metals involved in the galvanic assemblage.

2 Experimental

SUS304 stainless steel (18Cr-8Ni) and SS400 low carbon steel specimens (1cm x 1cm, thickness 0.3 cm) were used as working electrodes for the determination of cathodic and anodic polarization curves, respectively. The electrochemical runs were performed in 3.5% wt NaCl aqueous solution inside an autoclave, under purified CO_2 gas saturation. The solution was renewed with a flow rate of 0.6 lt/h. Potentials were measured, and are referred to in the text, versus a Ag/AgCl, 0.1 M KCl reference electrode (0.040 V *vs. SCE* at 10°C).

The polarization curve measurements were run at low scan rate (2 mV/min), after 24 h and 120 h of immersion in the solution. The temperature was varied from 50°C to 150°C for different experiments, under a pressure of 130 kgf cm^{-2}.

Fig. 1 shows a schematic experimental cell corresponding to the galvanic corrosion measurements. The two materials, SUS304 and SS400, were divided into

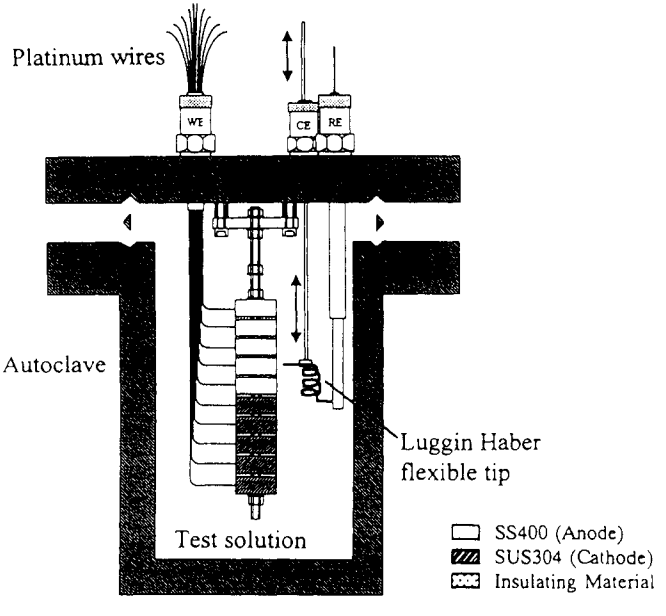

Figure 1. Diagram of the experimental arrangement for galvanic measurements.

sections insulated from each other. A platinum wire, which could be connected directly or via a current-measuring instrument to corresponding wires from other sections, was attached to each section. The Luggin-Haber capillary tip was flexible and its height inside the cell was externally controlled to set it nearer the electrode section under study (0.05 cm). Thus, the total galvanic current between the two materials as well as the individual current to and from each section could be measured. Potential and galvanic current density distributions over the material surfaces were measured after 24 h of immersion in 3.5% NaCl solution at 50°C.

3 Analysis by boundary element method

The results of polarization measurements were incorporated into boundary conditions, and the distributions of current and potential within the solvent and its surface were analyzed by the boundary element method.

3.1 Formulation of boundary element method

The boundary element method has been extensively described in textbooks by Brebbia[12,13]. Now, only a brief presentation of the method will be given.

Provided there is not storage or discharge of ions within the solvent, the electric potential ϕ corresponding to a domain Ω within the solvent should satisfy

$$\nabla^2 \phi = 0 \quad \text{(Laplace's equation)} \qquad \text{in } \Omega \qquad (1)$$

If the solvent is surrounded by the boundary Γ_1 characterizated by an electric potential ϕ_0, the boundary Γ_2 characterizated by a current density q_0 through the boundary, the anodic boundary Γ_{3a} and the cathodic boundary Γ_{3c}, the boundary conditions are given by

$$\phi = \phi_0 \qquad \text{on } \Gamma_1 \qquad (2)$$

$$q[=-k(\partial \phi / \partial n)] = q_0 \qquad \text{on } \Gamma_2 \qquad (3)$$

$$\phi = f_a(q) \qquad \text{on } \Gamma_{3a} \qquad (4)$$

$$\phi = f_c(q) \qquad \text{on } \Gamma_{3c} \qquad (5)$$

Here, k is the solution conductivity, and $\partial/\partial n$ indicates the derivative in the outer normal direction to the surface. $f_a(q)$ and $f_c(q)$ are the non-linear functions indicating polarization curves of anode and cathode, respectively.

Considering two points, P and Q within the domain Ω or its surface $\Gamma (= \Gamma_1 + \Gamma_2 + \Gamma_{3a} + \Gamma_{3c})$, the fundamental solution of the eqn (1) is called $\phi^*(P,Q)$. The source point is located at Q[13]. Both sides in eqn (1) are multiplied by $\phi^*(P,Q)$ and Q is set on Γ to consider the integration over the boundary. Integrating by parts twice, the following boundary integral formula can be obtained

$$k\, c\, \phi(Q) + \int_\Gamma \phi(P)\, q^*(P,Q)\, d\Gamma = \int_\Gamma q(P)\, \phi^*(P,Q)\, d\Gamma \qquad (6)$$

where $q^*(P,Q) = -k(\partial \phi^*(P,Q)/\partial n)$, and c is a constant[13]. The boundary Γ is divided into N elements, and the values of ϕ and q are assumed to be constant on each element and equal to the value at the middle point (node) of the element. Then, the following set of equations is obtained, expressed in matrix form for the N nodes as

$$[G]q^n = [H]\,\phi^n \tag{7}$$

Here, ϕ^n and q^n are the vector of the values of ϕ and q at the nodes and the matrix [G] and [H] are given by references Nos. 12 and 13.

Considering eqns (2) to (5), it can be perceived that the contents of q^n or ϕ^n involves some known factors. By removing such known factors to the right hand side and the unknown factors to the left hand side, eqn (7) can now be rewritten as

$$[A]\{x_1, \ldots x_i, \ldots x_r : q_1, \ldots q_i, \ldots q_s\} = [B]\{b_1, \ldots b_i, \ldots b_r : f_1(q_1), \ldots f_i(q_i), \ldots f_s(q_s)\} \tag{8}$$

Here, b_i corresponds to the value of the known factors of ϕ^n or q^n on the $\Gamma_1 + \Gamma_2$ boundary, while x_i is the unknown factor of b_i, and q_i represents the contents of q^n on the $\Gamma_{3a} + \Gamma_{3c}$ boundary, while $f_i(q_i)$ is the $f_a(q_i)$ or $f_c(q_i)$ that corresponds to q_i.

Because the matrix eqn (8) is in the form of nonlinear algebraic equations, it becomes necessary to calculate repeatedly to solve x_i and q_i. Initial values for x_i and q_i were tentatively set at random and the difference between both sides of eqn (8) was calculated. To reduce that difference, the Newton-Raphson iterative numerical procedure was employed to set the modified values of x_i and q_i. These modified values were substituted into the eqn (8) again. This procedure was repeated until the difference between both sides reached within preset tolerance.

4 Results and discussion

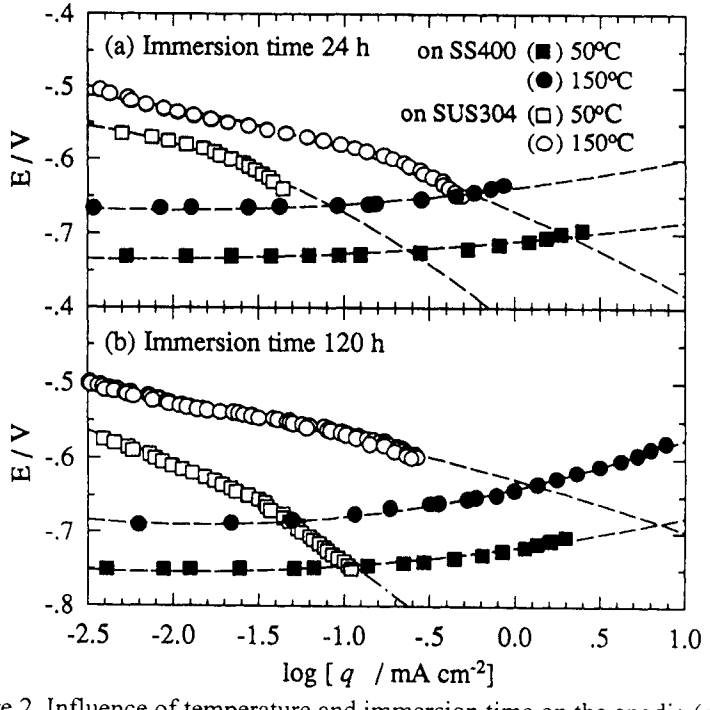

Figure 2. Influence of temperature and immersion time on the anodic (on SS400 carbon steel) and cathodic (on SUS304 stainless steel) polarization curves.

Before the equations are solved, the boundary conditions must be established. The conditions used in the actual calculations correspond to the geometry in Fig. 1. The boundary conditions on the metal surfaces are given by the relationship between potential and current density, derived from experimental polarization curves.

4.1 Polarization curve measurements

SUS304 and SS400 polarization curves were recorded at different temperatures, after 24 h and 120 h of immersion in 3.5% NaCl solution. Corrosion potentials shifted to more positive values as temperature increased and current density profiles depended on both temperature and immersion time in the solution (Figs. 2a and 2b). All the polarizarion results could be properly described by the expression:

$$f(q) = A (\log q)^2 + B (\log q) + C \qquad (9)$$

where A, B and C are fit parameters, depending on the kinetics involved in the electrode process. The optimal set of fit parameters was calculated and Table 1 shows their dependencies with the experimental variables. Assumed polarization curves in the actual potential region were drawn if necessary by extrapolation of the polarization curves using eqn (9) (dotted lines in Figs. 2a and 2b).

Table 1 - Temperature (°C) and immersion time (h) dependence of the fitting parameters of eqn (9).Using q in mA cm^{-2}, $f_a(q)$ and $f_c(q)$ are in mV.

		SS400			SUS304	
i) 24 h	A	B	C	A	B	C
50°C	4.7	21.3	-709.9	-29.9	-182.7	-824.2
150°C	7.6	30.5	-637.8	-14.0	-98.3	-669.5
ii) 120 h						
50°C	8.4	33.7	-720.2	-28.9	-216.5	-924.1
150°C	14.1	52.5	-640.2	-5.7	-62.9	-627.8

4.2 Galvanic current measurements

Galvanic current density was measured on the SS400-SUS304 couple, after 24 h of immersion in 3.5% NaCl solution at 50°C. The galvanic current density varied over the metal surfaces and the maximum galvanic corrosion rates for both cathodic and anodic electrodes were located in the joint of the metallic couple (Fig. 3). Differences in measured results form one section to the next can be explained by arbitrary variations in the surface conditions between the sections (differences in oxide properties of the stainless steel and in oxides and rust on the carbon steel). Lack of good adherence between the insulator material and the metallic elements may also cause ignorance of the exact electrode area.

4.3 Analysis conditions and analysis results

The boundary Γ was divided into 70 elements, corresponding 20 to the cathodic

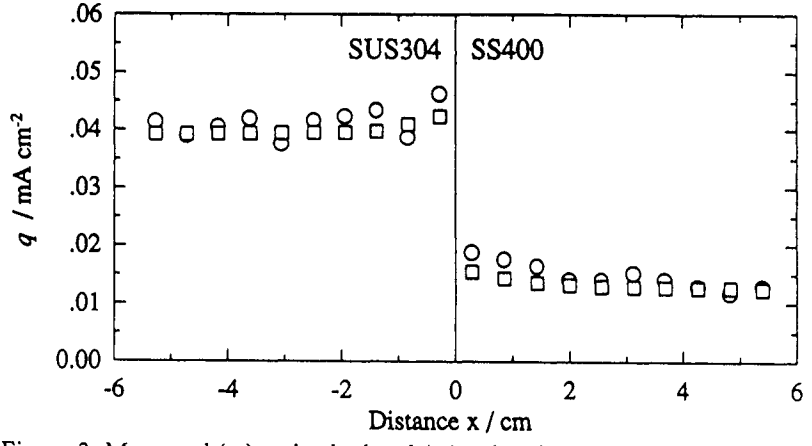

Figure 3. Measured (O) and calculated (□) galvanic current distribution as a function of distance from the contact plane between SS400 and SUS304.

stainless steel surface, 20 to that of the carbon steel, and the others to that of the solution. $f_a(q)$ and $f_c(q)$ were expressed by eqn (9) and the fitting parameters given in Table 1. Analytical results of the anodic and cathodic current density q are shown in Fig. 3, together with the experimental results. The results of the analysis correspond relatively well to the results of the experiments.The distribution of potentials ϕ within the solvent was also obtained through an inner point calculation, and the results are shown in Fig. 4.

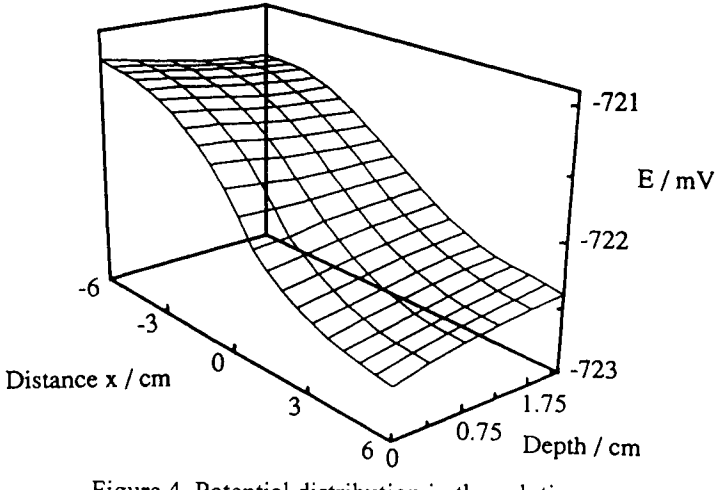

Figure 4. Potential distribution in the solution.

4.4 Convergence of solutions in the boundary element analysis

Analyzing with the boundary element method around the joint sections of anode and cathode, the current density changes drastically according to the different elemental spacing divisions. Then, the spacing around the joint sections was deliberately

varied to investigate the convergence of the solutions. The conditions were the same as in section 4.3, except that the analysis was made on anodic and cathodic continuous substances under various different elemental spacing divisions (Fig.5).

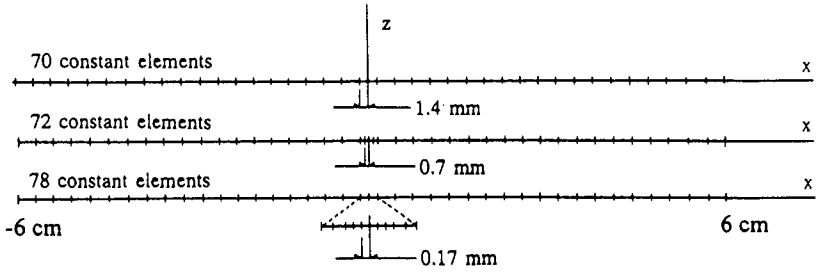

Figure 5. Boundary element discretizations for the surface of the galvanic couple.

The results for current density and potential distributions on the anode and cathode for several elemental spaces are presented in Figs. 6a and 6b. As spacing in cathodic and anodic sections gets narrower and in detail, the values of the electric current densities at the joint sections go upward. Therefore, to obtain the peak values, it should be necessary to undertake very narrow elemental spacing division. However, the current density and the potential around the locations centering in each respective element are obtained at nearly the same values whether the spacing is relatively rough or detailed (Figs. 6a and 6b). Thus, although the analysis is made on rough spacing, the potential at the joint sections can be sought from the inner settings, and more precise peak values of both cathodic and anodic current densities can be obtained from the experimental polarization curves (Figs. 2).

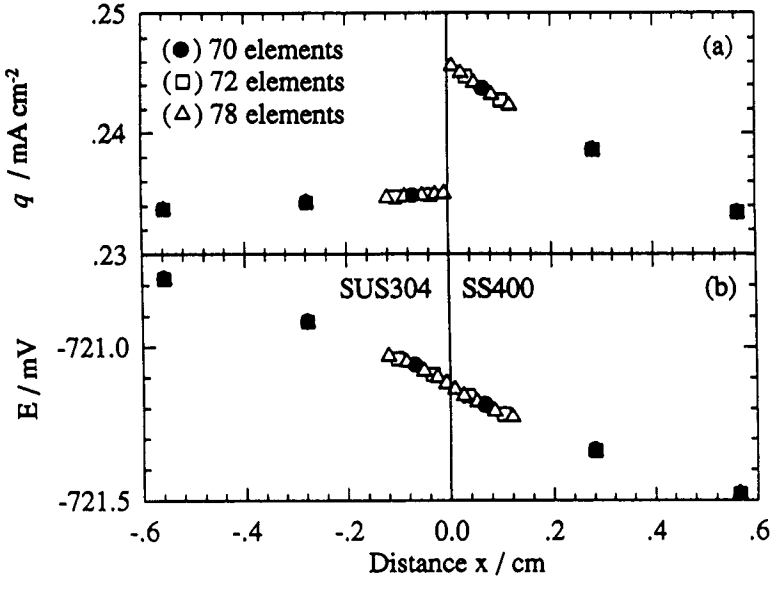

Figure 6. Convergence of numerical solutions of current density and potential distributions around the joint sections.

4.5 The influence of the substance division in the measured current density

To measure current density distribution on a metallic electrode in a galvanic couple, it is necessary to divide such substance into several elements and to separate each piece from the others with an insulating material. The current densities thus measured should be similar to those corresponding to the continuous distribution of the substance itself. Then, in this section, the number of spacing divisions was fixed, but the ratio of the thicknesses of divided specimen and insulating material was intentionally varied to undergo the boundary element analysis. All the other analytical conditions were the same as in the previous chapter.

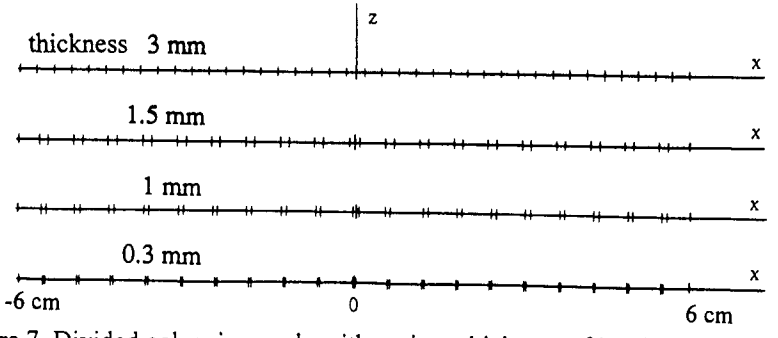

Figure 7. Divided galvanic couple with various thickness of insulating material.

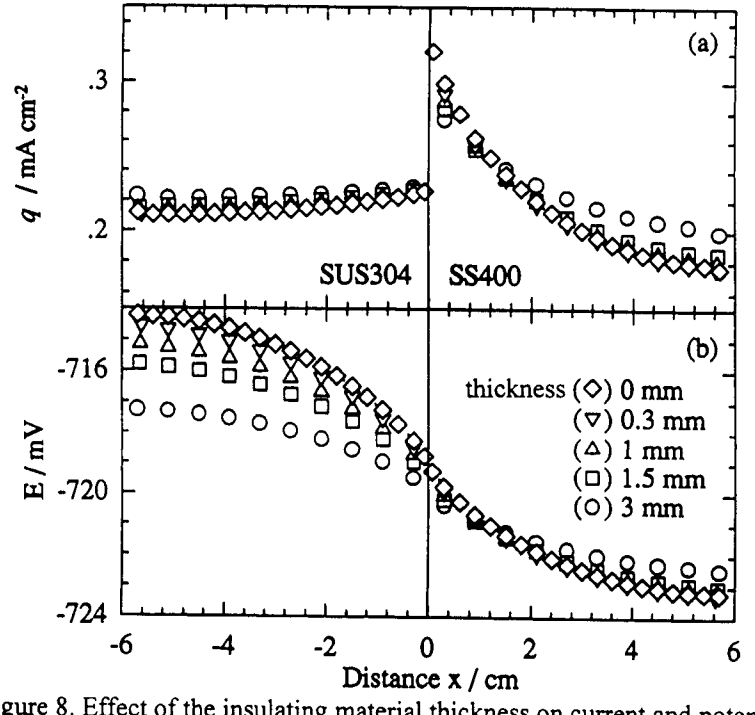

Figure 8. Effect of the insulating material thickness on current and potential distributions on the galvanic couple.

Fig. 7 shows the scheme of the different material thickness used. The results of calculations are presented in Figs. 8a and 8b.

From these results, clearly it is not possible to obtain the continuous values of the current density and potential distribution of a substance, unless the thickness of the insulating material is sufficiently narrow. But, as long as the thickness of the insulating substance is narrow enough, even if the spacing of the divided specimen is relatively wide, it is possible to obtain nearly approximate values.

4.6 Immersion time and temperature effects

To use the experimental ensemble developed for the galvanic measurements shown in Fig. 1 was not possible for long immersion times or high temperatures. The deterioration of the electrode in extreme corrosion conditions was advanced and the insulation between the different elements could not be ensured. Then, a prediction of galvanic results was made using the boundary element method and the different polarization curve data obtained for SS400 and SUS304 at different immersion times and temperatures (Table 1).

The results of the calculations are shown in Fig. 9 for 150°C. The cathodic current on SUS304 is more evenly distributed than the anodic current on the SS400. The reason for this is the higher slope of the polarization curve of the cathodic reaction on SUS304 than that corresponding to the anodic curve on SS400. Changes in the slope with the temperature also explain the fact that the current density and potential were much more evenly distributed for the lower temperatures.

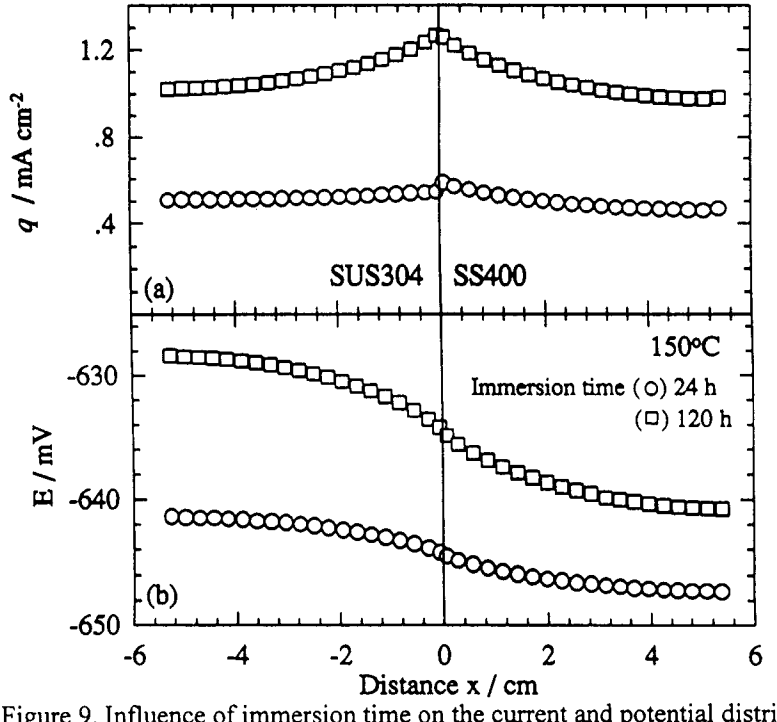

Figure 9. Influence of immersion time on the current and potential distributions at 150°C predicted by the boundary element method.

5 Conclusions

Corrosion of the SS400 carbon steel-SUS304 stainless steel couple in 3.5% NaCl solution has been analyzed. The experimental results were: *(i)* polarization curves of each component of the couple at different temperatures and immersion times; and *(ii)* the anodic and cathodic current density distributions across the galvanic couple.

The potential distribution within the electrolyte was described by the Laplace's equation with nonlinear boundary conditions, which were enforced based on the experimentally determined polarization curves. The Newton-Raphson iterative numerical procedure was employed to solve this boundary value problem. Good agreement was found between calculated and measured galvanic current densities.

It was shown that although solutions convergence is obtained only as the spacing gets narrower, the values at the joint corresponding to the continuous distributions could be accurately estimated from relatively rough spacing. Further, as result of dividing an electrode in several elements to measure its current density distribution, provided that the thickness of insulating material is narrow enough, the results of the measurements are comparable with the expected from a continuous distribution. Galvanic results for high temperatures and high immersion times in the solution were also successfully simulated.

References

1. H.P. Hack (Editor), *Galvanic Corrosion ASTM STP 978*, ASTM, Philadelphia, 1988.
2. J.T. Waber and M. Rosenbluth, *J.Electrochem.Soc.*, 1955, **102**, 344.
3. E. Kennard and J.T. Waber, *J.Electrochem.Soc.*, 1970, **117**, 880.
4. P. Doig and J. Flewitt, *J.Electrochem.Soc.*, 1979, **126**, 2057.
5. R. Strommen and A. Rodland, *CORROSION/80*, Preprint No. 241, NACE, Houston, Texas, 1980.
6. R.G. Kasper and M.G. April, *Corrosion*, 1983, **39**, 181.
7. E.A. DeCarlo, *Materials Performance*, 1983, **22**, 38.
8. D.J. Danson and M.A. Warne, *CORROSION/83*, Preprint No. 211, NACE, Houston, Texas, 1983.
9. C.A. Brebia and S.M. Niku, *Proceedings of the 7th Int. Conf. on Offshore Mechanics and Arctic Engineering*, pp.111-122, Houston, Texas, 1988.
10. E. Bardal, R. Johnsen and P.O. Gartland, *Corrosion*, 1984, **40**, 628.
11. S. Aoki, K. Kishimoto, K. Yoshibe and M. Miyasaka, *J.Soc.Mater.Science Japan*, 1986, **35**, 394.
12. C.A. Brebbia, *The Boundary Element Method for Engineers*, Pentech Press, London, 1978.
13. C.A. Brebbia and S. Walker, *Boundary Element Techniques in Engineering*, Newnes-Butterworths, London, 1980.